

# Chemically Doped Random Network Carbon Nanotube p–n Junction Diode for Rectifier

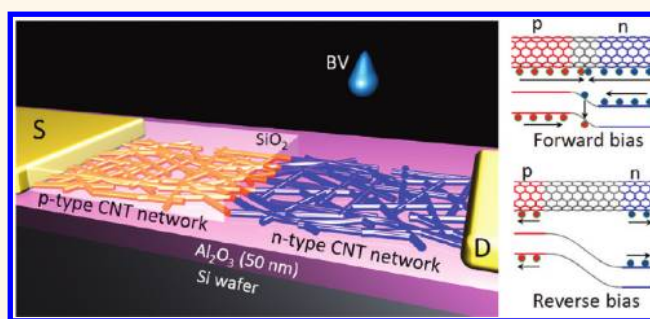
Chandan Biswas,<sup>†</sup> Si Young Lee,<sup>‡</sup> Thuc Hue Ly,<sup>‡</sup> Arunabha Ghosh,<sup>†</sup> Quoc Nguyen Dang,<sup>‡</sup> and Young Hee Lee<sup>†,‡,§,\*</sup>

<sup>†</sup>SKKU Advanced Institute of Nanotechnology, <sup>‡</sup>WCU Department of Energy Science, <sup>§</sup>Department of Physics, Sungkyunkwan University, Suwon 440-746, Republic of Korea

The prospects of modern semiconductor device physics rely on the control of carrier types, carrier concentration, and mobility. However, in order to perform desired complex circuitry operation, unipolar p-type and n-type and p–n junction devices are required. Furthermore, high carrier mobility is a prior condition for high-speed devices operated in a wide range of frequency signal processing. Single-walled carbon nanotubes (SWCNTs) are a one-dimensional (1D) class of material for building electronic devices due to their extraordinary electronic properties such as high mobility ( $\sim 10^5$  cm<sup>2</sup>/V s),<sup>1</sup> on–off current ratio ( $>10^5$ ),<sup>2</sup> and current carrying capacity ( $>10^9$  A/cm<sup>2</sup>).<sup>3,4</sup> A variety of devices, based on the integration of individual SWCNTs, have been demonstrated, including field effect transistors (FETs),<sup>2</sup> diodes,<sup>5–9</sup> logic circuit elements,<sup>10</sup> optical emission devices,<sup>11,12</sup> and chemical sensors.<sup>13</sup> However, a SWCNT rectifier operated in a wide range of frequencies is yet to be demonstrated.

The semiconducting SWCNTs in general show unipolar p-type behavior under ambient conditions.<sup>2,4,10</sup> Various chemical and nonchemical doping strategies have been applied to convert from p-type to n-type SWCNTs.<sup>14–17</sup> The p–n junction SWCNT diode using type conversion mechanism has been reported previously.<sup>5–9</sup> High leakage current and low diode rectification have often been observed under reverse bias conditions due to the poor doping ability of the previously used dopants.<sup>6,8,9</sup> A more effective doping control is required to have better diode characteristics. The key issue behind fabricating a high-performance rectifier device with a high-frequency input signal process using a SWCNT p–n junction diode is to have an efficient and stable doping strategy of SWCNT-type conversion.

## ABSTRACT



Semiconductors with higher carrier mobility and carrier density are required to fabricate a p–n junction diode for high-speed device operation and high-frequency signal processing. Here, we use a chemically doped semiconducting single-walled carbon nanotube (SWCNT) random network for a field effect transistor (FET) and demonstrate a rectifier operated at a wide range of frequencies by fabricating a p–n junction diode. The p–n diode was fabricated by using a pristine p-type SWCNT-FET where half was covered by SiO<sub>2</sub> and the other half was chemically doped by using benzyl viologen molecules, which was converted into an n-type channel. The half-wave rectifier of the random network SWCNT p–n junction diode clearly highlights the device operation under high input signal frequencies up to 10 MHz with very low output distortion, which a commercial silicon p–n junction diode cannot access. These results indicate that the random network SWCNT p–n junction diodes can be used as building blocks of complex circuits in a range of applications in microelectronics, optoelectronics, sensors, and other systems.

**KEYWORDS:** carbon nanotube · chemical doping · p–n junction · diode · rectifier

In order to achieve a high-performance rectifier device operated in a wide range of frequency input signals, both polarities of the SWCNT (p-type and n-type) should have high carrier mobilities and comparable on–off ratios.<sup>18</sup> Recent investigations show a stable n-type chemical dopant without degrading its semiconductor properties using electron-donating viologen and NADH molecules.<sup>19,20</sup> This provides an opportunity to develop a realistic high-performance

\* Address correspondence to leeyoung@skku.edu.

Received for review September 2, 2011 and accepted October 31, 2011.

Published online October 31, 2011  
10.1021/nn203391h

© 2011 American Chemical Society

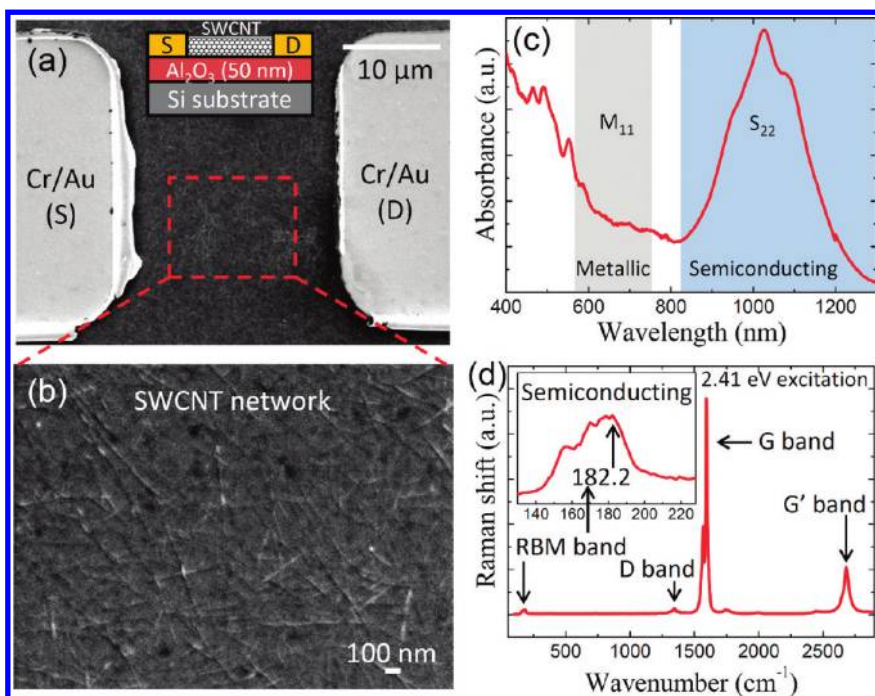


**Figure 1.** (a) Scanning electron micrograph of the SWCNT FET device. The figure inset represents the cross sectional schematic of the device. (b) High-resolution SEM micrograph of uniform SWCNT random network used for the FET devices. (c) Absorption spectroscopy of the separated semiconducting SWCNTs. Broad metallic and semiconducting bands are shown by shaded areas. (d) Raman spectroscopy of the SWCNT used for the FET devices. Figure inset shows the RBM mode in a magnified scale. Excitation energy of 2.41 eV was used.

rectifier device. Although an individual CNT was used to demonstrate a diode,<sup>5,6</sup> random network CNTs are preferred due to the facile fabrication process. The latter involves metallic channels that degrade the device performance.<sup>9</sup> Therefore, separated semiconducting channels are preferred for high-performance device operation. To our knowledge, there has been no report that uses exclusively a semiconducting SWCNT random network channel in fabricating diodes.

In this report, the separated semiconducting SWCNTs (96% purity) were used as a channel material for FET devices. The FET performance of the doped n-type semiconducting SWCNT network was not degraded due to the use of benzyl viologen (BV) as a stable and efficient chemical dopant. Half of the pristine p-type SWCNT random network channel was converted into n-type channel to form the SWCNT p–n junction diode. The combination of the semiconducting SWCNTs and stable BV dopant facilitated a high on–off ratio and similar current levels between p-channel and n-channel in the diode, which is a critical condition for minimizing leakage current and high rectifying efficiency in the rectifier. We demonstrate that the fabricated SWCNT rectifier shows a wide range of input frequency response up to 10 MHz, in good contrast with the commercial Si diode.

## RESULTS AND DISCUSSION

Carbon nanotube FETs were fabricated using random network semiconducting SWCNTs. A separated

semiconducting SWCNT solution was spin-coated on top of a Si/Al<sub>2</sub>O<sub>3</sub> substrate (Figure 1a).<sup>10</sup> The semiconducting SWCNTs over metallic SWCNTs in the random network were characterized by absorption and Raman spectroscopy. The SWCNT lengths of several hundred nanometers were uniformly and randomly distributed on the channel area, as shown in Figure 1b. The van Hove singularity transition associated with semiconducting S<sub>22</sub> peaks was clearly visible with a negligible metallic M<sub>11</sub> peak (Figure 1c) similar to the previous investigations.<sup>21</sup> The semiconducting properties of the SWCNT network were also verified with Raman spectroscopy (Figure 1d). Clearly distinguishable G', G, and D bands were observed near 2685, 1592, and 1345 cm<sup>-1</sup>, respectively. A significantly low D/G intensity ratio verifies good quality of the SWCNT with fewer defects. The radial breathing mode (RBM) near 150–200 cm<sup>-1</sup> (inset of Figure 1d) was observed, which is a characteristic of semiconducting SWCNTs.<sup>22</sup>

Figure 2a represents the transfer characteristics of the random network SWCNT FET devices. Among 300 FETs, all the devices showed high on–off ratios greater than 10<sup>3</sup>, which is ascribed to the use of semiconducting SWCNTs and mobilities greater than 2 cm<sup>2</sup>/(V s).<sup>10</sup> This high mobility is better than thin film amorphous Si devices (<0.1 cm<sup>2</sup>/(V s)).<sup>23</sup> Figure 2a is a typical FET device, which was obtained from high CNT density in solution,<sup>10</sup> revealing clear semiconducting p-type behavior with an on–off ratio of >10<sup>3</sup> and hole mobility of 7.2 cm<sup>2</sup>/(V s). The threshold voltage was observed

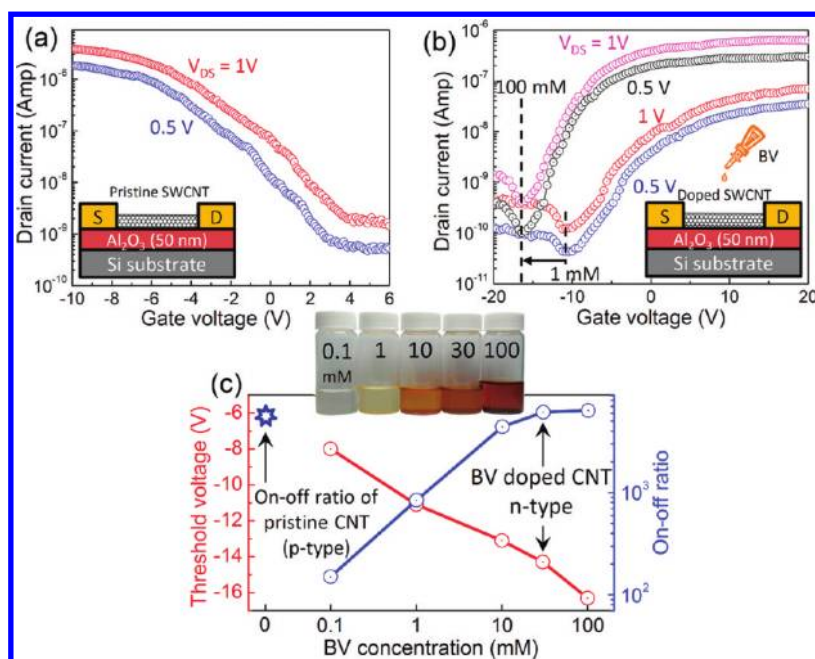


**Figure 2.** Electrical characterizations of p-type and n-type SWCNT-FET devices: (a) Transfer characteristics of the pristine p-type SWCNT-FET device. Figure inset represents the schematic diagram of the device. (b) Transfer characteristics of chemically doped n-type SWCNT-FET device with different BV doping concentrations. Different source–drain voltages were also used for comparison. (c) Threshold voltage shift and on–off ratio of doped n-type CNT FETs with different BV concentrations. The inset is a photograph of the BV solutions at different concentrations as designated.

near a gate voltage of 4 V. Lowering the source–drain voltage decreases the drain current level without reducing the on–off ratio. BV is an efficient charge dopant molecule that can effectively donate negative charges to SWCNT upon attachment on the surface and induces type conversion of SWCNTs from p-type to n-type by dropping a BV solution on the surface of the SWCNT, where viologen molecules donate electrons to compensate hole current and further to the empty conduction band of  $S_{11}$  and  $S_{22}$  of semiconducting SWCNTs to increase electron current in the FET device.<sup>19,24</sup> The pristine p-type SWCNTs were converted into n-type, as shown in Figure 2b. The threshold voltage in this case was downshifted. As the BV doping concentration increased from 1 mM to 100 mM (Figure 2c), the on current (electron) level increased and the threshold voltage was consistently downshifted. The electron mobility with BV doping of 1 mM was  $5.1 \text{ cm}^2/(\text{V s})$  and increased to  $6.3 \text{ cm}^2/(\text{V s})$  at 100 mM. These values (n-type, electron mobilities) are comparable with p-type (hole) mobilities, which verifies no degradation of carrier mobilities due to chemical doping. As the BV concentration increased, the threshold voltage was shifted to higher negative gate voltage and the on–off ratio increased initially and was saturated at high BV concentration (Figure 2c). It is noted that the on current level of the n-type transistor is similar to that of the pristine p-type transistor. This demonstrates the efficiency of the BV dopant for type conversion to n-type.

Figure 3a is the schematic model of a SWCNT p–n junction diode device based on random network SWCNTs. Half of the SWCNT-FET channel was encapsulated with a 300 nm thick  $\text{SiO}_2$  layer, which preserves the pristine p-carrier-type SWCNT, while the other half was doped with BV to form a p–n junction diode. Figure 3b is the SEM micrograph of the top view of the diode device in which the encapsulated  $\text{SiO}_2$  layer is visible, covering half of the channel length. Figure 3c represents the  $I$ – $V$  characteristics of the diode device that operates at  $\pm 2 \text{ V}$ , where the current flows at forward bias and no current was allowed to flow in the reverse bias condition in both p-type and n-type biasing polarities. This is a clear demonstration of the diode operation of the SWCNT p–n junction device.<sup>25</sup> The variation in the output characteristics of the random network SWCNT diode under different BV doping concentrations was investigated. With increasing BV concentration, the on current level increased slightly with a well-defined off current, while threshold voltage was not altered appreciably, as shown in Figure 3d. The device-to-device variation in on–off current levels with changing BV doping concentrations is presented in Figure S1. The on current level increased in all the devices as the BV doping concentration increased, whereas the off current level remained constant independent of doping concentration. Increasing BV concentration alters the n-type depletion region to modify the electric field gradient at the junction. As a consequence, the on current level was altered. Since the p-type region is fixed at constant doping

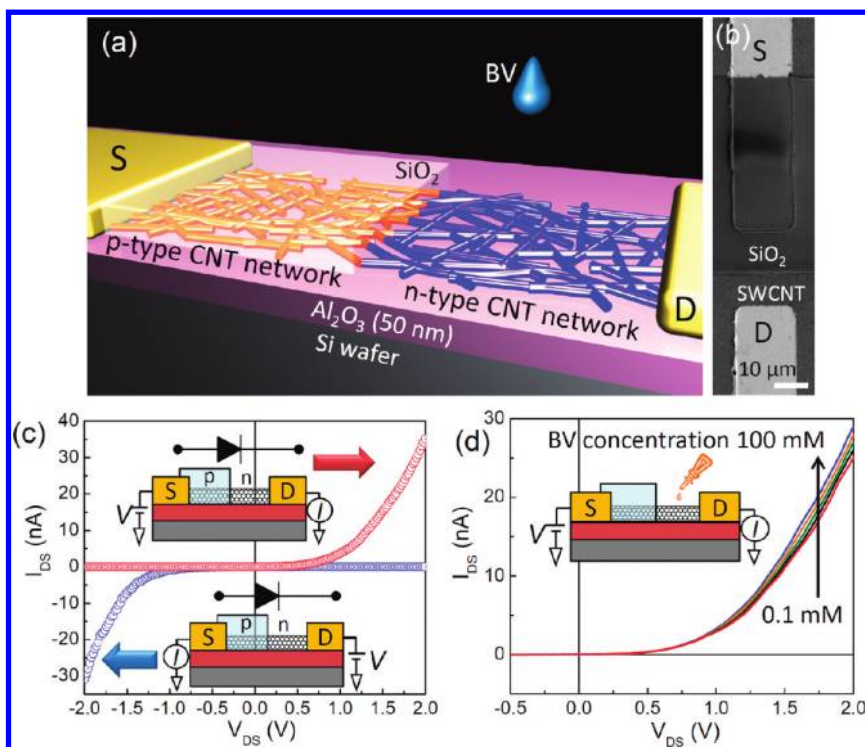


**Figure 3.** Device structure and electrical characterization of random network SWCNT p–n junction diode: (a) schematic model of SWCNT p–n junction diode based on a random network of SWCNTs. Half of the SWCNT FET channel was encapsulated with a SiO<sub>2</sub> layer (see SEM micrograph in (b)), whereas the rest of the channel was chemically doped with BV to form a p–n junction between the source and drain electrodes. (c) *I*–*V* characteristics of random network SWCNT p–n junction diode in which half of the p-type CNT was converted into n-type with a BV doping of 30 mM concentration. (d) *I*–*V* characteristics of random network SWCNT p–n junction diode with different n-type dopant concentrations.

concentration, the balance of the majority current on both sides plays a role in maximizing the diode current.

Crucial device parameters can be evaluated by comparing the asymmetric nonlinear current–voltage relationship of the p–n junction diode. In order to investigate our random network SWCNT p–n junction diode operation, we have plotted the output *I*–*V* characteristics in absolute semilogarithmic current scale and fitted with the conventional p–n junction diode equation as follows (Figure 4a).<sup>25</sup>

$$I_{DS} = I_S(e^{V_{DS}/nk_B T} - 1) \quad (1)$$

where  $I_{DS}$  is the collected current from the diode under applied voltage  $V_{DS}$ ,  $I_S$  is the reverse bias saturated leakage current,  $n$  is the ideality factor of the diode,  $k_B$  is the Boltzmann constant, and  $T$  is the temperature. For an ideal diode, the ideality factor becomes unity. However, in reality, the ideality factor value is larger<sup>26,27</sup> than 1 and could take a value between 1 and 2 for the case of silicon diodes.<sup>25</sup> Our random network SWCNT diode *I*–*V* characteristics fit with the diode equation (eq 1) with an  $I_S$  value near  $4.7 \times 10^{12}$  A and an ideality factor of 4.8 (Figure 4a). Under reverse bias conditions, the diffusion potential barrier height between the p-type and n-type side becomes too high to flow a significant current through the device. However, under forward bias conditions ( $V_{DS} > 0$ ) the diffusion potential

barrier is lowered, which causes a large gradient of carriers to diffuse as from one side to the other side of the diode, as illustrated in the band diagram of the inset. At the higher forward bias region, the experimental curve deviates from theoretical values (Figure 4b). This is a common phenomenon in planar diodes, as significant voltages are dropped near to contact of the metal electrodes and semiconducting SWCNTs. Increasing the contact resistance between electrodes and SWCNTs increases the diode series resistance, due to which the experimented current level deviates from the diode equation. Further investigation reveals the experimental random network SWCNT diode *I*–*V* output current matches with an ideal diode equation ( $n = 1$ ) only up to very small forward bias voltages (Figure 4b). The forward biased *I*–*V* characteristics of real p–n diodes are diminished at the higher voltage region by a high injection of carriers followed by the series resistance of the diode. These effects were illustrated by the schematic *I*–*V* characteristics of a silicon p–n diode in Figure 4c.<sup>25</sup> The *I*–*V* characteristics are sketched on a semilogarithmic current scale, and four different regions can be distinguished. At the initial stage of the forward bias, the current is dominated by the trap-assisted recombination in the depletion region, designated as “depletion region recombination”, in which the curve has an ideality factor more than 1 in

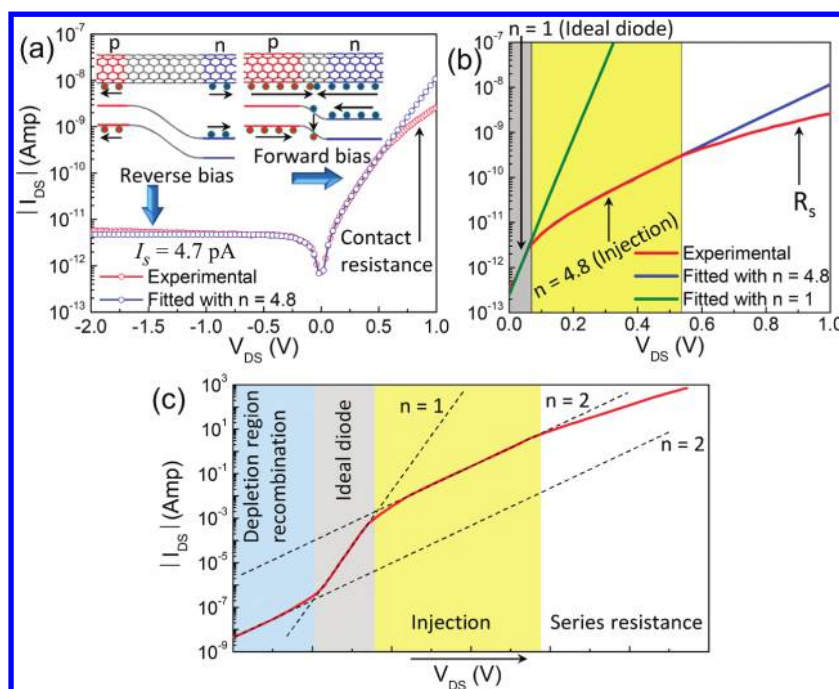


Figure 4. (a)  $I$ - $V$  curve of the CNT p-n junction diode plotted in absolute magnitude of the current and fitted with eq 1 with an ideality factor ( $n$ ) of 4.8. The inset shows the band diagram during forward and reverse bias near the vicinity of the p-n junction. (b)  $I$ - $V$  curve of the random network SWCNT p-n junction diode fitted with ideal diode equation and eq 1 (with  $n = 4.8$ ) at different voltage ranges. (c) Schematic  $I$ - $V$  plot of a typical silicon p-n junction diode fitted with different ideality factors representing different conduction regions. The x-axis arrow represents the direction of increasing source drain bias.

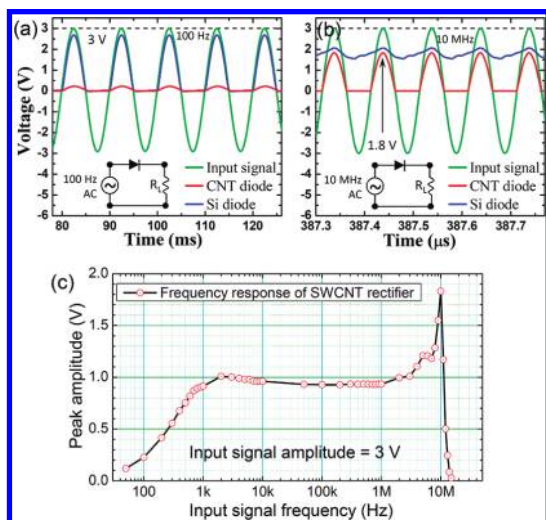


Figure 5. Input and output characteristics of a SWCNT rectifier device: (a, b) Input and output characteristics of a SWCNT half-wave rectifier operated at a frequency of (a) 100 Hz and (b) 10 MHz input ac signals and compared with a commercial Si rectifier diode (1N4005). Input signal amplitude was maintained constant at 3 V. (c) Output peak amplitude variations of the SWCNT rectifier with different input signal frequencies (at 3 V input signal amplitude).

the case of the Si diode. After this region, the current of the diode increases exponentially with increasing magnitude of the applied voltage. This region is referred to as the “ideal diode” region with the value of  $n = 1$ . Interestingly, the depletion region was not visible in our random network SWCNT diode. This implies that the

depletion region is negligibly narrow or no recombination occurs for carrier injection. Because of this fact, the injection of the carrier is more severely restricted at higher voltage due to the limited diffusion, giving rise to a higher ideality factor of 4.8. Minimizing the series resistance including contact resistance could significantly improve the performance of the random network SWCNT p-n junction diode. We emphasize here that our molecular doping using BV is quite stable under ambient conditions.<sup>19</sup> Our p-n diode fabricated with BV showed good environmental stability with similar diode characteristics with a negligible current level after 12 days, in good corroboration with the previous report (see Supporting Information (SI) S2).

The most primary and important application of a diode is its rectification performance. The basic use of a rectifier is to transform an alternating current (ac) signal to a direct current (dc) signal. Figure 5 illustrates the rectification performance and frequency response of the random network SWCNT diode. The performance of a basic half-wave rectifier constructed using a single random network SWCNT diode was compared with a commercial silicon p-n junction rectifier diode (1N4005). Both rectifiers were operated with identical input signal at a frequency of 100 Hz with an amplitude of 3 V (Figure 5a). Both SWCNT and silicon diodes show good rectification behavior by carrying the positive ac signal with low signal distortion, while demonstrating zero bias at negative ac signals. The rectified amplitude is relatively small in the case of the random network

SWCNT diode. The situation becomes different at a high input frequency signal of 10 MHz (Figure 5b). The output signal of the rectifier silicon diode was distorted, and the rectification amplitude was reduced with respect to the high-frequency sinusoidal inputs due to the low carrier mobility of silicon.<sup>28,29</sup> However, very high carrier mobilities of SWCNT<sup>1</sup> enables fast carrier conduction, resulting in good rectifier performance with very low distortion even under high-frequency input signals. Thus, p–n junction diode materials with high carrier mobility are required for high-frequency operations. The rectifier performance of other types of nonrectifier planar silicon diodes (such as high-frequency diodes, band switching diodes, small signal diodes) was investigated and compared (see SI S3). The output peak amplitude also improves under high-frequency input signal up to 1.8 V. The input signal frequency response on the output peak amplitude of the SWCNT rectifier is plotted in Figure 5c. At low input signal frequency, the SWCNT rectifier showed a low output peak amplitude due to presumably high contact resistance between SWCNTs and the metal electrode and SWCNT–SWCNT network junction resistance. Nevertheless, the distortion of the waveform is much smaller than those of Si diodes shown in S3. The output peak amplitude increased smoothly at the low-frequency region, was saturated near 1 kHz, and remained almost constant up to 1 MHz. The peak amplitude increased rapidly after 1 MHz, reaching maximum amplitude at 10 MHz, followed by a fast

decay at higher frequency. This high-frequency cut provides another opportunity for the SWCNT rectifier to be used as a frequency limiter.

## CONCLUSION

The fabrication and performance characterization of a chemically doped SWCNT random network based p–n junction diode has been demonstrated here. The semiconducting SWCNTs were exclusively used to fabricate a random network channel with high yield of fabrication and high on–off ratio. While the pristine p-type SWCNTs were used, half of the device was converted to n-type SWCNT by chemical doping with BV dopant to form a p–n junction diode. Similar levels of on–off ratio and on current to p-type SWCNT channels were obtained in the n-type SWCNT channel with high mobilities of 5–8 cm<sup>2</sup>/(V s). Fitting the *I*–*V* characterization with the ideal diode equation reveals a negligibly narrow depletion region, resulting in large carrier injection. The half-wave rectifier device constructed with random network SWCNT diodes operates at higher input signal frequencies up to 10 MHz with low input–output signal distortion in which commercial silicon diodes fail. These results highlight the application opportunity of the random network semiconducting SWCNT p–n junction diodes to be used in high-frequency signal processing, high-speed microelectronics circuitry, optoelectronics, sensors, and other systems such as frequency limiters and frequency band-pass filters.

## METHODS

The semiconducting SWCNTs separated from metallic SWCNTs by a density gradient ultracentrifugation method were purchased from NanoIntegris Inc. The separated SWCNTs were then dispersed in *N*-methylpyrrolidinone by a three-hour sonication (120 W, 35 kHz) followed by a centrifugation at 10 000 rpm for two hours. An insulating layer of 50 nm alumina was deposited on a bare silicon wafer by atomic layer deposition. The 100  $\mu$ L SWCNT solution was spin-coated on top of the alumina to have uniform high density SWCNT network formation. The source and drain electrodes (5 nm Cr followed by 50 nm gold) were then deposited by an electron beam evaporator under a conventional photolithography mask pattern. The 1,1'-dibenzyl-4,4'-bipyridinium dichloride (benzyl viologen) powder (0.04 mg) with a purity of 96.0% (purchased from Fluka) was dissolved in 10 mL of water followed by an addition of 10 mL of toluene, resulting in a biphasic solution. The reducing agent of 200 mM sodium borohydride was added to the solution and kept for 24 h, and the reduced BV was segregated to toluene from water. The concentration of the BV in toluene can be altered by changing the initial BV concentration in water. This BV solution dispersed in toluene was used as the n-type dopant of SWCNTs. In order to convert p-type SWCNTs into n-type SWCNTs, one drop of 5  $\mu$ L of BV solution was used with different concentrations. ac/dc measurements were conducted using a semiconductor characterization system (model 4200, Keithley Instruments Inc.).

*Acknowledgment.* This work was supported by the Star Faculty program (2010-0029653), International Research & Development Program (2011-00242), and WCU program (R31-2008-10029) of the NRF of Korea funded by MEST.

*Supporting Information Available:* The document contains supporting data and text. This material is available free of charge via the Internet at <http://pubs.acs.org>.

## REFERENCES AND NOTES

- Dürkop, T.; Getty, S. A.; Cobas, E.; Fuhrer, M. S. Extraordinary Mobility in Semiconducting Carbon Nanotubes. *Nano Lett.* **2004**, *4*, 35–39.
- Javey, A.; Kim, H.; Brink, M.; Wang, Q.; Ural, A.; Guo, J.; McIntyre, P.; McEuen, P.; Lundstrom, M.; Dai, H. High-[kappa] Dielectrics for Advanced Carbon-Nanotube Transistors and Logic Gates. *Nat. Mater.* **2002**, *1*, 241–246.
- Yao, Z.; Kane, C. L.; Dekker, C. High-Field Electrical Transport in Single-Wall Carbon Nanotubes. *Phys. Rev. Lett.* **2000**, *84*, 2941–2941.
- Javey, A.; Guo, J.; Wang, Q.; Lundstrom, M.; Dai, H. Ballistic Carbon Nanotube Field-Effect Transistors. *Nature* **2003**, *424*, 654–657.
- Lee, J. U.; Gipp, P. P.; Heller, C. M. Carbon Nanotube p-n Junction Diodes. *Appl. Phys. Lett.* **2004**, *85*, 145–145.
- Yang, M. H.; Teo, K. B. K.; Milne, W. I.; Hasko, D. G. Carbon Nanotube Schottky Diode and Directionally Dependent Field-Effect Transistor Using Asymmetrical Contacts. *Appl. Phys. Lett.* **2005**, *87*, 253116–253116.

7. Li, Y. F.; Hatakeyama, R.; Shishido, J.; Kato, T.; Kaneko, T. Air-Stable p-n Junction Diodes Based on Single-Walled Carbon Nanotubes Encapsulating Fe Nanoparticles. *Appl. Phys. Lett.* **2007**, *90*, 173127–173127.
8. Zhou, C.; Kong, J.; Yenilmez, E.; Dai, H. Modulated Chemical Doping of Individual Carbon Nanotubes. *Science* **2000**, *290*, 1552–1555.
9. Zhou, Y.; Gaur, A.; Hur, S.-H.; Kocabas, C.; Meitl, M. A.; Shim, M.; Rogers, J. A. p-Channel, n-Channel Thin Film Transistors and p–n Diodes Based on Single Wall Carbon Nanotube Networks. *Nano Lett.* **2004**, *4*, 2031–2035.
10. Lee, S. Y.; Lee, S. W.; Kim, S. M.; Yu, W. J.; Jo, Y. W.; Lee, Y. H. Scalable Complementary Logic Gates with Chemically Doped Semiconducting Carbon Nanotube Transistors. *ACS Nano* **2011**, *5*, 2369–2375.
11. Misewich, J. A.; Martel, R.; Avouris, P.; Tsang, J. C.; Heinze, S.; Tersoff, J. Electrically Induced Optical Emission from a Carbon Nanotube FET. *Science* **2003**, *300*, 783–786.
12. Mueller, T.; Kinoshita, M.; Steiner, M.; Perebeinos, V.; Bol, A. A.; Farmer, D. B.; Avouris, P. Efficient Narrow-Band Light Emission from a Single Carbon Nanotube p-n Diode. *Nat. Nanotechnol.* **2010**, *5*, 27–31.
13. Kong, J.; Franklin, N. R.; Zhou, C.; Chapline, M. G.; Peng, S.; Cho, K.; Dai, H. Nanotube Molecular Wires as Chemical Sensors. *Science* **2000**, *287*, 622–625.
14. Biswas, C.; Lee, Y. H. Graphene vs Carbon Nanotube in Electronic Devices. *Adv. Funct. Mater.* **2011** in press.
15. Shim, M.; Javey, A.; Shi Kam, N. W.; Dai, H. Polymer Functionalization for Air-Stable n-Type Carbon Nanotube Field-Effect Transistors. *J. Am. Chem. Soc.* **2001**, *123*, 11512–11513.
16. Siddons, G. P.; Merchin, D.; Back, J. H.; Jeong, J. K.; Shim, M. Highly Efficient Gating and Doping of Carbon Nanotubes with Polymer Electrolytes. *Nano Lett.* **2004**, *4*, 927–931.
17. Klinke, C.; Chen, J.; Afzali, A.; Avouris, P. Charge Transfer Induced Polarity Switching in Carbon Nanotube Transistors. *Nano Lett.* **2005**, *5*, 555–558.
18. Kumngern, M.; Knobnob, B.; Dejhan, K. High Frequency and High Precision CMOS Half-Wave Rectifier. *Circuits Syst. Signal. Process.* **2010**, *29*, 815–836.
19. Kim, S. M.; Jang, J. H.; Kim, K. K.; Park, H. K.; Bae, J. J.; Yu, W. J.; Lee, I. H.; Kim, G.; Loc, D. D.; Kim, U. J.; *et al.* Reduction-Controlled Viologen in Bisolvent as an Environmentally Stable n-Type Dopant for Carbon Nanotubes. *J. Am. Chem. Soc.* **2009**, *131*, 327–331.
20. Kang, B. R.; Yu, W. J.; Kim, K. K.; Park, H. K.; Kim, S. M.; Park, Y.; Kim, G.; Shin, H. J.; Kim, U. J.; Lee, E. H.; *et al.* Restorable Type Conversion of Carbon Nanotube Transistor Using Pyrolytically Controlled Antioxidizing Photosynthesis Coenzyme. *Adv. Funct. Mater.* **2009**, *19*, 2553–2559.
21. Arnold, M. S.; Green, A. A.; Hulvat, J. F.; Stupp, S. I.; Hersam, M. C. Sorting Carbon Nanotubes by Electronic Structure Using Density Differentiation. *Nat. Nanotechnol.* **2006**, *1*, 60–65.
22. Dresselhaus, M. S.; Dresselhaus, G.; Saito, R.; Jorio, A. Raman Spectroscopy of Carbon Nanotubes. *Phys. Rep.* **2005**, *409*, 47–99.
23. Moore, A. R. Electron and Hole Drift Mobility in Amorphous Silicon. *Appl. Phys. Lett.* **1977**, *31*, 762–762.
24. Kim, K. K.; Yoon, S.-M.; Park, H. K.; Shin, H.-J.; Kim, S. M.; Bae, J. J.; Cui, Y.; Kim, J. M.; Choi, J.-Y.; Lee, Y. H. Doping Strategy of Carbon Nanotubes with Redox Chemistry. *New J. Chem.* **2010**, *34*, 2183–2183.
25. Neudeck, G. W.; Pierret, R. F. The PN Junction Diode. In *Modular Series on Solid State Devices*; Addison-Wesley Publishing Company, Inc.: United States of America, 1989; Vol. 2.
26. Shah, J. M.; Li, Y. L.; Gessmann, T.; Schubert, E. F. Experimental Analysis and Theoretical Model for Anomalously High Ideality Factors ( $n \gg 2.0$ ) in AlGaIn/GaN p-n Junction Diodes. *J. Appl. Phys.* **2003**, *94*, 2627–2627.
27. Zhu, D.; Xu, J.; Noemaun, A. N.; Kim, J. K.; Schubert, E. F.; Crawford, M. H.; Koleske, D. D. The Origin of the High Diode-Ideality Factors in GaInN/GaN Multiple Quantum Well Light-Emitting Diodes. *Appl. Phys. Lett.* **2009**, *94*, 081113–081113.
28. Masetti, G.; Severi, M.; Solmi, S. Modeling of Carrier Mobility against Carrier Concentration in Arsenic-, Phosphorus-, and Boron-Doped Silicon. *IEEE Trans. Electron Devices* **1983**, *30*, 764–769.
29. Caughey, D. M.; Thomas, R. E. Carrier Mobilities in Silicon Empirically Related to Doping and Field. *Proc. IEEE* **1967**, *55*, 2192–2193.